

# Dynamical implications of the orientation of atmospheric eddies: a local energetics perspective

By M. CAI<sup>1\*</sup>, S. YANG<sup>2</sup>, H. M. VAN DEN DOOL<sup>2</sup> and V. E. KOUSKY<sup>2</sup>, *Department of Meteorology, Florida State University, Tallahassee, FL 32306, USA; NOAA's Climate Prediction Center, 5200 Auth Road, Camp Springs, MD 20746, USA*

(Manuscript received 25 April 2006; in final form 18 September 2006)

## ABSTRACT

A local quasi-geostrophic energetics analysis indicates that within the jet core, low-frequency (LF) eddies behave baroclinically essentially the same as high-frequency (HF) eddies. They both have a westward tilting vertical structure and both grow baroclinically by transporting heat poleward and by converting eddy potential energy to kinetic energy. However, the difference in the horizontal orientations of HF and LF eddies has several important implications to their amplitude and peak locations, as well as their interaction with stationary waves. The barotropic decay of meridionally elongated HF eddies tends to terminate the growth of HF eddies beyond the jet exit region. The barotropic growth of the zonally elongated LF eddies not only ensure a continuous growth of LF eddies in the jet exit region, but also results in a new baroclinic growth of LF eddies farther downstream due to the presence of the west–east temperature contrast associated with stationary waves. The continuous growth of LF eddies due to both barotropic and baroclinic processes in the jet exit region is consistent with the facts that LF eddies reach maximum variability farther downstream of the two major jet streams and that the LF variability is much stronger than HF eddies.

The results of energetics analysis are confirmed by the feedback analysis, showing that HF eddies, being dominated by meridional orientations, mainly act to maintain (damp) stationary waves by locally enhancing (reducing) north–south gradient of the height (temperature) field near the jet core regions. The zonally elongated LF eddies, on the other hand, act to primarily reduce the zonal gradient associated with stationary waves both barotropically and baroclinically.

## 1. Introduction

The variability of the tropospheric atmosphere is associated with atmospheric eddies of various temporal and spatial scales. These eddies play an important role in determining the state of atmospheric circulation patterns through their interaction with the time-mean flow and through the interactions among themselves and transporting momentum and heat across latitudes (e.g., Hoskins et al., 1983; Plumb, 1986; Lau, 1988; Cai and Mak, 1990a; Dole and Black, 1990; Cai and van den Dool, 1991, 1992; Sheng and Derome, 1991; Branstator, 1995; Cuff and Cai, 1995; Black, 1998; Chang et al., 2002; and references therein). It is known that atmospheric eddies of different time scales have different characteristics both in terms of their preferred location with respect to the background flow and their preferred orientations or shapes. The variability of synoptic-scale high-frequency (HF) eddies exhibits maximum amplitude downstream of the

time mean jet streams while the sub-seasonal low-frequency (LF) variability peaks further downstream and further poleward of the jet streams (Blackmon et al., 1977). This is illustrated in Fig. 1, which shows the climatological (1948–2000) December–January–February (DJF) stationary waves along with the local standard deviations of HF (<10 d) and LF (10–90 d) transient eddies derived from NCEP/NCAR reanalysis 500-hPa geopotential height field.

Part of intraseasonal LF eddies result from atmospheric responses to the forcings associated with tropical SST anomalies of ENSO or midlatitude SST anomalies (e.g. Held et al., 1989; Ting and Held, 1990; Ting, 1994; Peng and Whitaker, 1999; Watanabe and Kimoto, 2000). Another important source of the atmospheric LF variability is local barotropic instability of a zonally varying background state, explaining why the maximum LF variability is observed at some distance downstream of the jet core (e.g. Simmons et al., 1983; Mak and Cai, 1989). It also has been recognized that HF eddies play a crucial role in generating/maintaining LF variability while being organized by LF variability (e.g., Egger and Schilling, 1983; Lau and Holopainen, 1984; Lau, 1988; Cai and Mak, 1990b; Cai and van den Dool,

---

Corresponding author.  
e-mail: cai@met.fsu.edu  
DOI: 10.1111/j.1600-0870.2006.00213.x

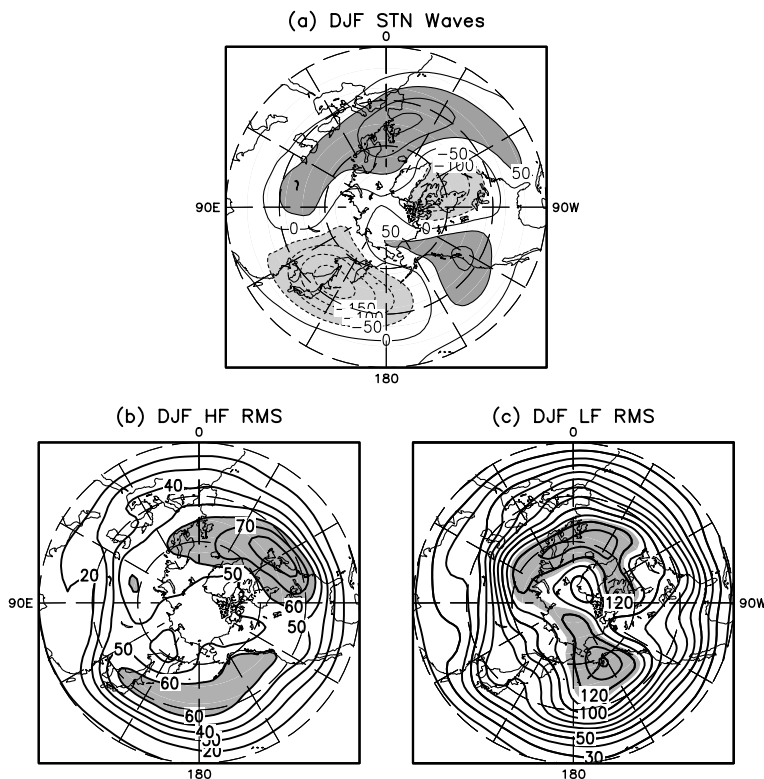


*Fig. 1.* December–January–February mean patterns of (a) stationary waves, (b) standard deviation of HF (<10 d) variability and (c) standard deviation of LF (10–90 d) variability calculated from the 500 hPa geopotential height of the NCEP–NCAR reanalysis and averaged for the time period 1948–2000. The unit is meters. Shadings indicate values larger than 60 m in panel (b) and 115 m in panel (c).

1991; Lau and Nath, 1991; Robinson, 1991; Branstator, 1995; Cuff and Cai, 1995; Limpasuvan and Hartmann, 1999, 2000; Chang et al., 2002).

The horizontal shape or orientation of transient eddies can be defined by the major axis of the velocity correlation tensor or the E-vector of transient eddies (Hoskins et al., 1983; Mak and Cai, 1989; Cai, 1992; Whitaker and Dole, 1995; Black and Dole, 2000; Iacono, 2002; and Cai, 2003). Hoskins et al. (1983) showed a significant disparity between LF and HF eddies in terms of their dominant orientations, namely that the HF eddies are primarily meridionally elongated whereas the LF eddies are zonally elongated. As pointed out by Mak and Cai (1989) and Cai (1992) and discussed more thoroughly in Cai (2003), the orientation and location of eddies, relative to the background deformation flow, determine the direction and rate of barotropic energy conversion between the mean flow and transients. The kinetic energy exchange between the background flow and eddies essentially is through a continuous deformation of eddies due to the straining mechanism of the background deformation field as first pointed out by Shutts (1983) and discussed in more details in Farrell (1989), Cai (1992), and Iacono (2002) in the context of non-modal growth of localized eddies embedded in a background deformation field.<sup>1</sup>

<sup>1</sup>Cai (2003) rectified an error in Cai (1992). Refer to Fig. 5 of Cai (2003) for details.

One of the widely used diagnostics tools for studying interactive relationships of transient eddies and the time mean flow is the Eliassen–Palm (E–P) flux analysis (e.g. Edmon et al., 1980; Andrews, 1983; Plumb, 1986). For a zonally averaged flow, the wave–mean flow interaction can be diagnosed using the E–P flux defined in the meridional–vertical plane based on a conservation relation (Edmon et al., 1980). The E–P flux itself, being proportional to the group velocity, is indicative of the direction of wave activity propagation and its convergence measures the forcing to the zonal-mean flow. The 2-D E–P flux vector has been extended to a 3-D flux vector that satisfies a conservation relation of a pseudo energy/momentum quantity for a zonally varying basic flow (Andrews, 1983; Plumb, 1986; Takaya and Nakamura, 2001). The diagnostics using an extended 3-D E–P flux vector in a conservation relation is appealing because the flux vector itself is indicative of wave activity propagation and its convergence is a measure of the down-gradient flux of potential vorticity by eddies which implies a net forcing to the mean flow. Therefore, in principle, such a wave-activity flux vector describes not only propagation of wave activities but also the locations where eddies interact with the mean flow. In the framework of the E–P flux, the baroclinic energy conversion from the mean flow to perturbation implies a source region of wave activities propagating upward whereas barotropic energy conversion from the eddy to the mean flow implies a source of wave activities propagating into the mean jet stream.

In this study, we will primarily use the quasi-geostrophic local energetics analysis to depict the relationship between atmospheric eddies of different temporal scale and localized time mean jet streams. In the literature, there are some debates about the arbitrariness of local energetics calculations. The arbitrariness of local energetics analysis arises only when one rewrites the energy conversion terms by invoking the chain rule, resulting in new terms that have zero global mean values but non-zero local values which are not uniquely defined. For example, the non-uniqueness would arise if one wishes to write the energetics conversion terms in the E–P flux form. Although the global mean calculation is identical, the local interpretation is very difficult. As discussed in Cai (2003), such arbitrariness does not exist if one starts from the original momentum and thermodynamic equations without adding or deleting any non-divergent terms into/from the equations. Mak and Cai (1989) and Cai and Mak (1990a) have demonstrated that such local energy calculation can exactly balance the terms on the right hand side with those on the left hand side of the local energetics equations. Furthermore, only through such a unique energetics partitioning, one can learn that the kinetic energy conversion from the mean flow to the perturbation flow is due to the basic deformation rather than the vorticity field (Mak and Cai, 1989; Cai, 1992). In particular, the statement that ‘*a barotropically unstable eddy has to lean against shear*’ should be rephrased as ‘*a barotropically unstable perturbation has to be elongated along the contraction axis of the basic deformation.*’

It should be pointed out that the local energetics analysis does not directly yield information about how disturbances would modify the mean state. A complementary diagnostics analysis, namely, ‘feedback analysis’ pioneered by Lau and Holopainen (1984), can be carried out to infer the potential modification to the basic state. Because the same dynamical quantities (i.e., eddies’ momentum/heat or potential vorticity fluxes) are involved in both diagnostics but with opposite sign, the energy conversion terms are complementary to feedback diagnostics (e.g., a positive energy conversion from the mean flow to perturbations would imply a negative feedback to the mean flow, and vice versa). In this paper, we will apply the feedback analysis to delineate the dynamically induced eddy forcing terms that act to maintain the mean state.

Given that atmospheric eddies of different time scales have different characteristics of preferred locations and orientations and that these characteristics are critical for determining the energy conversion between the eddies and the mean flow, one may ask the following questions: How does the orientation of transient eddies change with respect to the background flow? Can the preferred location of transient eddies (relative to the background flow) be partially explained by their dominant orientations? Does the difference in the orientation of eddies imply different interactions between eddies and the mean flow in both barotropic and baroclinic components? Do LF eddies also have a westward tilting vertical structure? Why do LF eddies tend to be

zonally oriented and HF eddies tend to be meridionally oriented? Compared to HF eddies, the nature of LF variability remains a less resolved problem in the overall dynamics of the atmosphere (Swanson, 2002). Particularly, there are only a few studies concerning the baroclinic characteristics of LF variability—most often the general description of ‘equivalent barotropic structure’ is used.

In this study, we will attempt to address these questions by calculating (i) the covariance matrices of eddy momentum flux (for determining the horizontal orientation) and heat flux (for determining the vertical tilting), (ii) the quasi-geostrophic local energetics and (iii) feedback tendency using the National Centers for Environmental Prediction (NCEP)–National Center for Atmospheric Research (NCAR) reanalysis data set spanning from 1948 to 2000 (Kalnay et al., 1996; Kistler et al., 2001). The NCEP/NCAR reanalysis enables us to revisit the earlier diagnoses (e.g. Hoskins et al., 1983; Lau and Holopainen, 1984; Dole and Black, 1990; Sheng and Derome, 1991) concerning the fundamental properties of LF and HF eddies using a long record data set that were not available in 1980s and early 1990s. We are particularly interested in studying the energetics properties of LF variability to examine their variations with respect to the zonally varying jet streams, using a long data set to supplement the many studies of the HF eddies using an equally long data set (Chang et al., 2002 and the references therein). In addition to depicting the variation of the preferred horizontal orientations and the local barotropic and baroclinic energetics of LF and HF eddies with respect the zonally varying jet streams, we are also interested in the vertical orientations in terms of the westward tilt of both LF and HF eddies.

The paper is divided into three sections. In the next section, we describe the data and analysis methods applied in this study. The results obtained will be presented in Section 3 and summarized in Section 4.

## 2. Data and analysis methods

In this study, we use the NCEP–NCAR reanalysis data set (Kalnay et al., 1996 and Kistler et al., 2001). We analyse the daily geopotential height, temperature, and vertical velocity at 500 hPa for the time period 1948–2000. For each field, we first calculate the mean value for each calendar day across all of 52 yr, resulting in 365 consecutive maps for each field. The daily annual cycle is obtained by applying a 31-d running-mean to these 365 maps. The daily transients are then obtained by subtracting the daily annual cycle from the original daily data. Next, we apply the Hanning filter (Hanning 1983) to the daily transients to acquire the HF and LF transients using the entire data set covering the period from January 1, 1948 to December 31, 2000. The HF and LF eddies analysed in this study are defined as the transients with time scales less than 10 d and in the 10-to-90 d band, respectively. Unless specified otherwise, the results shown in this paper are for the DJF period from 1948 to 2000.

Since our energetics analysis and transient eddy feedback calculations are done in the quasi-geostrophic framework, we use the geostrophic wind derived from the height field. It is of importance to point out that the 500 hPa analysis may not necessarily be representative of a vertical average. For example, barotropic energy conversion terms are largest at the upper levels whereas baroclinic energy conversion terms are dominant at the lower levels where the background baroclinicity is strongest. Because the vertical motion tends to have a maximum in the middle of the troposphere, the energy conversion term from eddy potential energy to eddy kinetic energy is representative at 500 hPa. Based on these factors, we argue that 500 hPa would be the best choice if only one-level of data is used. Moreover, the diagnostics analysis (such as local energetics and feedback calculations) using 500 hPa data is in accordance with a typical two-layer quasi-geostrophic model configuration. It should also be pointed out that the vertical propagation properties of transient eddies of different time scales cannot be addressed in detail with single level diagnostics although one can easily relate a poleward heat transport to an upward propagation of wave activities as defined by the E–P flux. Readers can consult with Plumb (1986) for detailed discussions on the vertical propagation properties of LF and HF eddies. Here we infer the vertical tilt from the horizontal phase difference between harmonic waves in temperature and height.

Following Mak and Cai (1989), for both HF and LF eddies, we have obtained the time mean maps of the following vertically averaged energy conversion terms using the data at 500 hPa only in accordance with a two-layer model configuration:

$$BT = C(K_{\text{bar}} - > K_{\text{transient}}) = C_0 \vec{E} \cdot \vec{D}$$

$$= C_0 \left\{ \frac{1}{2}(\overline{v'^2} - \overline{u'^2}) \left( \frac{\partial \bar{u}}{\partial x} - \frac{\partial \bar{v}}{\partial y} \right) + (\overline{-u'v'}) \left( \frac{\partial \bar{v}}{\partial x} + \frac{\partial \bar{u}}{\partial y} \right) \right\}, \quad (1)$$

$$BC = C(P_{\text{bar}} - > P_{\text{transient}}) = -C_2 \left( \overline{u'T'} \frac{\partial \bar{T}}{\partial x} + \overline{v'T'} \frac{\partial \bar{T}}{\partial y} \right), \quad (2)$$

$$PK = C(P_{\text{transient}} - > K_{\text{transient}}) = -C_1 (\overline{\omega'T'}), \quad (3)$$

where,  $(\bar{u}, \bar{v})$  are the climatological mean zonal and meridional geostrophic winds and  $\bar{T}$  is the climatological mean temperature field at 500 hPa and they are obtained by averaging the 31-d running-mean daily climatology data over the DJF period;  $\vec{V}' = (u', v')$  are the transient parts (either HF or LF eddies) of the 500-hPa geostrophic winds;  $\omega'$  and  $T'$  are the transient vertical motion and temperature at 500 hPa, respectively. The  $D$ -vector of the time mean flow and  $E$ -vector of transients are defined as  $\vec{D} = (\frac{\partial \bar{u}}{\partial x} - \frac{\partial \bar{v}}{\partial y}, \frac{\partial \bar{v}}{\partial x} + \frac{\partial \bar{u}}{\partial y})$  and  $\vec{E} = (\frac{1}{2}(\overline{v'^2} - \overline{u'^2}), \overline{-u'v'})$ , respectively. The overbar stands for an average over the DJF period from 1948 to 2000. The constants  $C_0$ ,  $C_1$  and  $C_2$  are

evaluated at 500 hPa, and are defined as

$$C_0 = \frac{P_{00}}{g}, \quad C_1 = \frac{2^{C_v/C_p} R}{g} \quad \text{and} \quad C_2 = \frac{2^{R/C_p}}{\left(-\frac{d\Theta}{dp}\right)} C_1, \quad (4)$$

where  $R$  is the gas constant for dry air,  $g$  the acceleration of gravity,  $C_p$  and  $C_v$  are the specific heat capacity of dry air at the constant pressure and volume, respectively,  $P_{00} = 1000$  hPa representing the mean sea level pressure, and  $-\frac{d\Theta}{dp}$  measures the mean atmospheric static stability in the extratropics, which has been set to be 3.5 K/100 hPa. The units of the energetics conversion terms defined in (1)–(3) are  $\text{W m}^{-2}$ , representing the vertically averaged energetics over the entire column of the atmosphere in accordance with a two-layer quasi-geostrophic model.

There are two noteworthy points. First, the barotropic growth/decay defined in eq. (1) is not applicable for an isotropic (or a circular) eddy. Using the conservation principle of ‘pseudoenergy wave activity’, Swanson et al. (1997) showed that an isotropic eddy can still experience a barotropic growth by decreasing its diameter when passing through a zonally varying background flow. Secondly, unlike the other two energy conversion terms, the PK term defined in (3) is not explicitly related to the mean jet stream. The PK term is the part of the pressure work that causes a vertical redistribution of mass. There exists the same energetics process for the jet stream itself, namely, the energy transfer between potential and kinetic energy of the mean flow associated with the secondary circulation which is positive in the jet entrance region and negative in jet exit region (e.g., Cressman 1981 and 1984).

The transient eddy feedback calculations are based on

$$\frac{\partial h}{\partial t} = \nabla^{-2} \left[ -\frac{f_0}{g} \nabla \cdot (\vec{V}' \zeta') \right], \quad (6)$$

$$\frac{\partial T}{\partial t} = -\nabla \cdot (\vec{V}' T'), \quad (7)$$

where  $\zeta'$  is transient eddy (either HF or LF) geostrophic vorticity and  $f_0$  is the Coriolis parameter at 45°N; and  $\frac{\partial h}{\partial t}$  and  $\frac{\partial T}{\partial t}$  stand for the geopotential height and temperature tendencies due to vorticity and heat flux convergences of transient eddies, respectively.

## 3. Results

### 3.1. Barotropic analysis

In this subsection, we discuss the results computed from eq. (1). Figure 2 shows the contraction axis of the winter season (DJF) climatological flow at 500 hPa, and the winter season climatological mean orientations of the major axis of HF and LF eddies. The angle of the contraction axis of the mean flow is

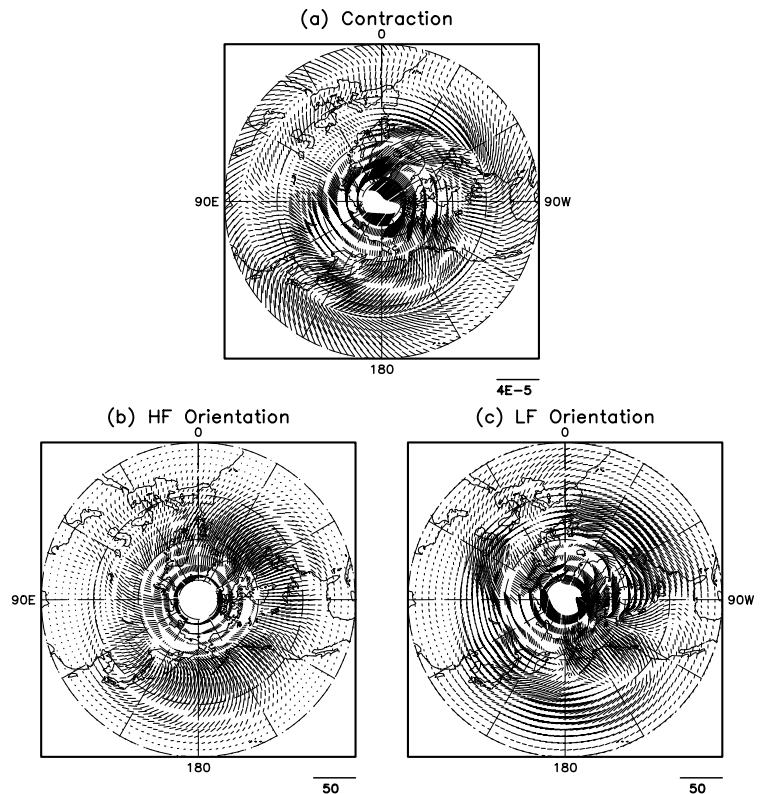


Fig. 2. Contraction axis orientation of the basic flow (a) and eddy orientations for HF transients (b) and LF transients (c). The orientation angle in panel (a) is calculated according to (8) and in (b) and (c) according to (9). The length of segments in (a) represents amplitude of the  $D$ -vector (in unit of  $s^{-1}$ ) and the length of segments in (b) and (c) corresponds to amplitude of  $E$ -vector (in unit of  $m^2s^{-2}$ ) evaluated for HF and LF transients, respectively. The unit length of segments is indicated by the length at the right bottom of each panel.

defined as

$$\text{contraction\_axis\_angle} = \frac{1}{2} \tan^{-1} \left( \frac{\frac{\partial \bar{v}}{\partial x} + \frac{\partial \bar{u}}{\partial y}}{\frac{\partial \bar{u}}{\partial x} - \frac{\partial \bar{v}}{\partial y}} \right) + 90^\circ. \quad (8)$$

And the mean orientation of the transient (HF in Fig. 2b and LF in Fig. 2c) eddies is

$$\text{eddy\_orientation\_axis\_angle} = \frac{1}{2} \tan^{-1} \left[ \frac{-\overline{u'v'}}{\frac{1}{2}(\overline{v'^2} - \overline{u'^2})} \right] + 90^\circ. \quad (9)$$

This figure provides a reference for our following discussion about the basic features of atmospheric eddies and their relationships with the background flow. Although the barotropic energy conversion term is explicitly expressed in terms of the inner product of the  $D$ -vector of the basic flow and the  $E$ -vector of the transient eddies, as shown in eq. (1), it is easy to examine the local barotropic energy conversion graphically from the local contraction axis of deformation of the basic flow and the orientation of the eddies as shown in Fig. 2. When the  $E$ -vector and  $D$ -vector point to the same direction, which implies a maximum positive barotropic energy conversion to transients from the mean flow, the eddy orientation is parallel to the contraction axis of the basic deformation. On the other hand, when the  $E$ -vector and  $D$ -vector point in the opposite direction, which implies a maximum negative barotropic energy conversion to transients from the mean

flow, the eddy orientation is perpendicular to the contraction axis or is parallel to the dilatation axis of the basic deformation.

The orientation of the contraction axis in the entrance region of a local jet core lies primarily along the north–south direction and it changes to the west–east orientation in the jet exit region (Fig. 2a). At the jet core, the shearing deformation is dominant and the corresponding contraction axis lies along the northwest–southeast (southwest–northeast) direction on the southern (northern) flank of the jet core. The orientation of HF eddies (Fig. 2b) is more or less perpendicular to the local contraction axis along the two major jet streams except in the jet entrance region and along the north edge of the jet core where the orientation of HF eddies is parallel to the contraction axis of the basic state. This implies that the HF eddies gain kinetic energy from the basic flow only in the jet entrance and along the north edge of the jet core and deposit kinetic energy into the basic flow mainly in the jet exit region, the southern flank, and the further north away from the jet core. Such a kinetic energy conversion from HF eddies to the jet stream is equivalent to the maintenance of the jet stream by transporting westerly momentum into the jet. The feature that the HF eddies draw kinetic energy from the background flow in the north edge of the jet core suggests that HF eddies tend to reduce the cyclonic shear along the jet core and effectively make the jet meridionally wider. On the other hand, the dominance of the west–east orientation of LF eddies (Fig. 2c) implies that LF eddies extract kinetic energy from the jet stream mainly in the exit region. It is also evident that

the orientation of LF eddies is nearly parallel to the contraction axis in the northern flank of the jet streams.

The inner product of the  $E$ -vector and  $D$ -vector, which gives rise to the kinetic energy conversion rate from the basic flow to transient eddies according to eq. (1), is mathematically equal to the sum of the product of the  $x$ -components and the product of the  $y$ -components of the two vectors. The contribution from the  $x$ -components, denoted as  $BT_b$ , is associated with the stretching deformation of the background flow. For a background flow that is non-divergent, we have

$$BT_b = C_0 \frac{(\overline{v^2} - \overline{u^2})}{2} \left( \frac{\partial \bar{u}}{\partial x} - \frac{\partial \bar{v}}{\partial y} \right) = 2C_0 \frac{(\overline{v^2} - \overline{u^2})}{2} \frac{\partial \bar{u}^*}{\partial x}, \quad (10)$$

where ‘\*’ denotes the departure from the zonal mean part of the flow. Therefore, the term  $BT_b$  depends primarily on the stationary wave components of the background flow.

The contribution from the product of the  $y$ -components of the  $E$ -vector and  $D$ -vector is related to the shearing deformation of the background flow, which can be rewritten as

$$\begin{aligned} C_0 \overline{(-u'v')} \left( \frac{\partial \bar{v}}{\partial x} + \frac{\partial \bar{u}}{\partial y} \right) \\ = C_0 \overline{(-u'v')} \frac{\partial [\bar{u}]}{\partial y} + C_0 \overline{(-u'v')} \left( \frac{\partial \bar{v}^*}{\partial x} + \frac{\partial \bar{u}^*}{\partial y} \right) \\ = BT_c + BT_d, \end{aligned} \quad (11)$$

where  $[\ ]$  stands for the zonal mean operator. It follows that the term  $BT_c$  is associated with the shearing deformation of the zonally averaged background flow whereas the term  $BT_d$  is related to the stationary-wave shearing deformation flow.

Plotted in panels (b), (c) and (d) of Figs. 3–4 are the terms  $BT_b$ ,  $BT_c$ , and  $BT_d$ , for HF (Fig. 3) and LF (Fig. 4), respectively. The sum of the terms  $BT_b$ ,  $BT_c$ , and  $BT_d$  is plotted in panel (a) of Figs. 3–4, which is the kinetic energy conversion rate from the basic flow to transient eddies. Such a partition of the barotropic energy conversion term between the zonally varying mean flow and transient eddies, which to our knowledge has not been done in the literature, would help us to relate the sources of atmospheric variability of different time scales to their dominant orientation with respect to the spatial variation of the deformation field associated with the climatological jet streams. From the perspective of the background flow, one can easily attribute the term  $BT_c$  to the energy conversion in the classic barotropic instability problem of a zonally uniform basic flow and the terms  $BT_b$  and  $BT_d$  to the zonal inhomogeneity of the background stretching and shearing deformation flow, respectively. From the perspective of eddy orientations, one can associate the terms  $BT_b$  with meridionally/zonally elongated and  $(BT_c + BT_d)$  with horizontally tilted eddies, respectively. Specifically, for meridionally/zonally elongated eddies (i.e.,  $\frac{1}{2} |(\overline{v^2} - \overline{u^2})| \gg |-\overline{u'v'}|$ ), the barotropic energy conversion tends to take place over the jet entrance/exit regions where the stretching deformation is

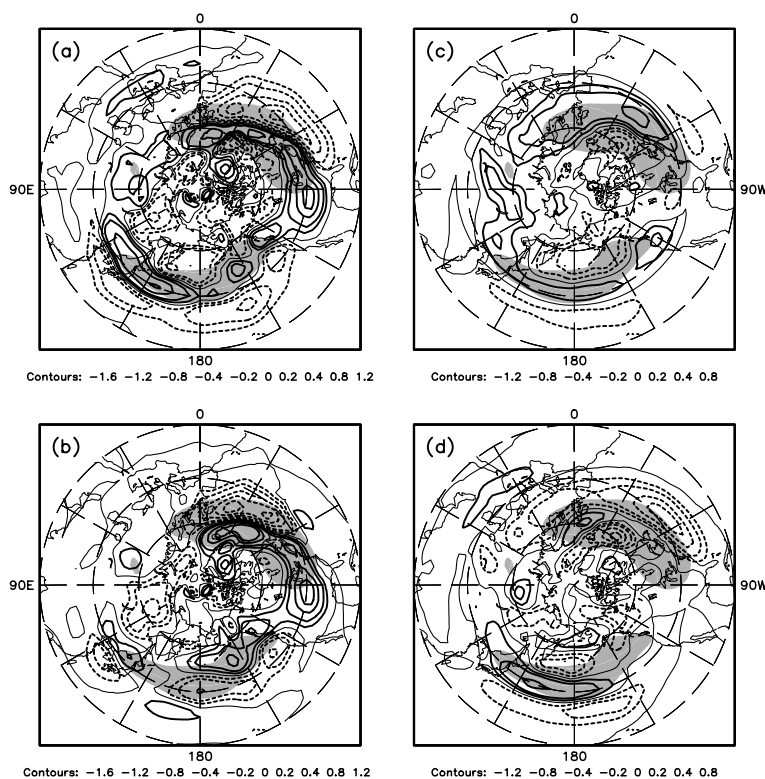


Fig. 3. Kinetic energy conversion rate (in units of  $\text{W m}^{-2}$ ) from the basic flow to HF transients: (a) total; (b) due to the stretching deformation; (c) due to the zonal mean shear deformation and (d) due to the wave portion of the shearing deformation (see text for the details of the partition of kinetic energy conversion rate). Shaded areas indicate the location of the storm tracks (HF standard deviation exceeds 60 m as shown in Fig. 1).

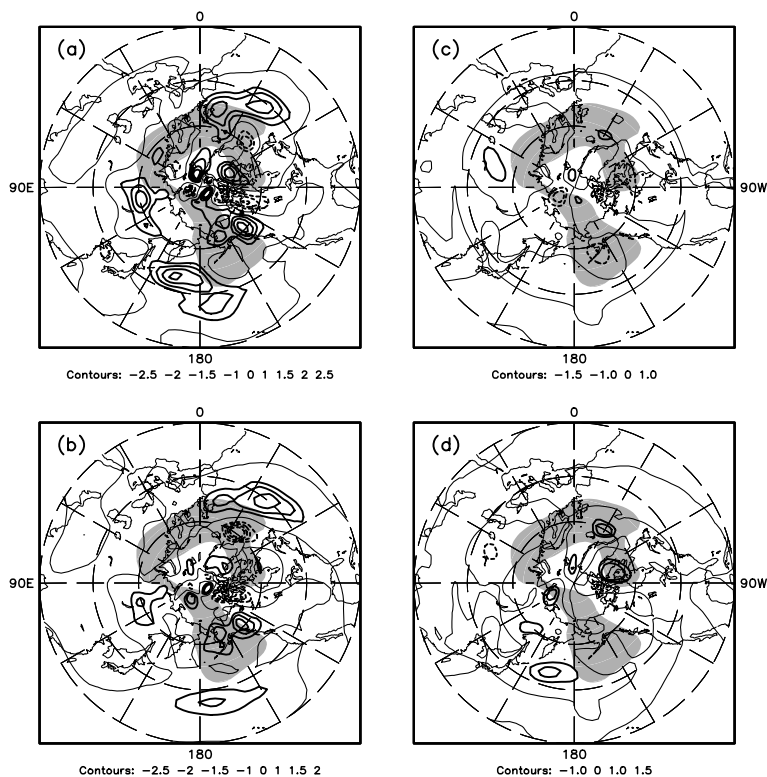


Fig. 4. Same as in Fig. 3, but for energy conversion rate from the basic flow to LF transients. Shaded areas indicate the regions where LF standard deviation exceeds 115 m as shown in Fig. 1.

dominant or the term  $BT_b$  is dominant. For horizontally tilted eddies (i.e.,  $|\frac{1}{2}(v'^2 - u'^2)| \sim | -u'v' | \neq 0$ ), the barotropic energy conversion tends to take place over the north and south flanks of the mid-latitude jet streams, and the terms  $BT_c$  and  $BT_d$  are dominant.

Figure 3a shows that the extraction of kinetic energy by HF eddies from the mean flow mainly occurs in the entrance region of the mean jet streams and along the north edge of the jet cores, in accordance with our graphical analysis derived from Fig. 2. To the south and further north of the jet cores and over the exit regions of the jet streams, HF eddies give energy back to the mean flow. Having primarily a meridionally elongated orientation, HF eddies extract kinetic energy through the stretching deformation from the mean flow in the jet entrance region and supply kinetic energy to the mean flow in the jet exit region (Fig. 3b). The slightly southwest–northeast orientation of otherwise meridionally elongated orientation helps HF eddies to extract kinetic energy through the shearing deformation along the north edge of the mid-latitude westerly jet belt (Fig. 3c and d). The alignment of the HF eddy orientation with the dilatation axis of shearing deformation results in a loss of kinetic energy of HF eddies to the mean flow along the north and south flanks of the jet core (Figs. 3c and d). In terms of momentum flux, HF eddies produce a net westerly momentum transport into the north and south flanks of the jet core and into the jet exit region and act to broaden the jet in the meridional direction and extend the jet in the downstream direction. Such a deduction about the

feedback of HF eddies on the mean flow can be independently verified from the direct calculation of the feedback tendencies induced by the transients as to be shown in Fig. 10.

Figure 4 shows characteristically different features for LF variability from those illustrated in Fig. 3 for the HF variability. Other than in the jet entrance region where LF eddies lose kinetic energy to the mean flow, LF eddies gain kinetic energy from the mean flow. The positive energy conversion from the mean flow is particularly pronounced along the poleward flank of the jet exit region where the stretching deformation is strongest and the contraction axis of the stretching deformation is nearly parallel to the zonally elongated LF eddies (Fig. 4b). The shear deformation associated with the zonally symmetric mid-latitude westerly belt contributes little to the barotropic energy process of LF eddies (Fig. 4c) whereas the shearing deformation associated with stationary waves acts as a supplementary energy source along the poleward flank of jet streams (Fig. 4d). Over the southern flank of the jet core, because the orientation of LF eddies lies nearly between the contraction and dilatation axes of the basic deformation field, there is little barotropic energy conversion from the mean flow to transients.

Figure 5 summarizes the main features of the observed HF and LF eddies orientations with respect to the mean jet stream, as well as their barotropic energetics shown in Figs. 2–4. Being meridionally elongated, HF eddies grow barotropically by extracting energy from the mean flow in the jet entrance region and near the north edge of the jet core. HF eddies elsewhere have their

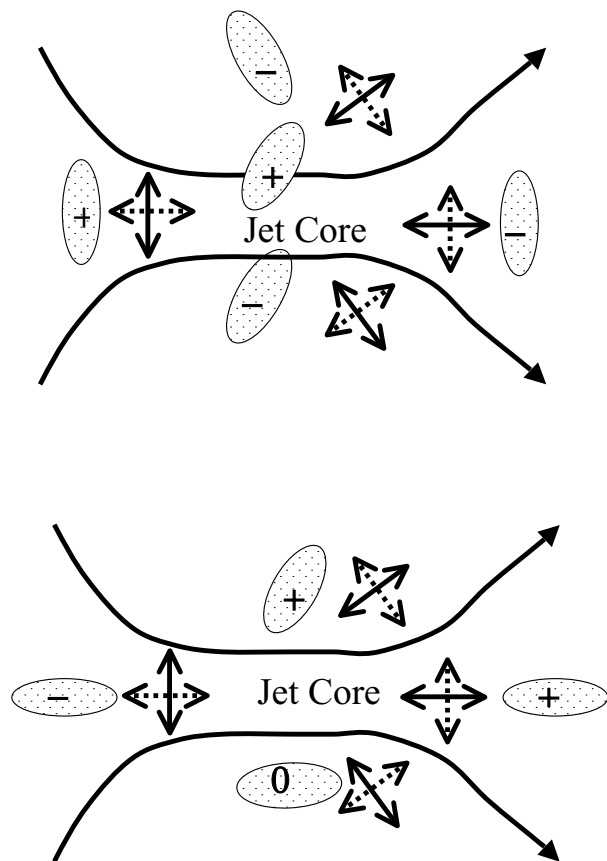


Fig. 5. Schematic diagram showing the variation of the dominant orientations (shaded ellipses) of the observed transient eddies with respect to the time mean jet stream (curves: basic streamfunction). (a) HF transients and (b) LF transients. The positive signs represent kinetic energy gained by the eddies from the basic flow; the negative signs represent loss of eddy energy to the basic flow; and '0' corresponds to the case of little barotropic energy exchange with the basic flow. The solid and dashed double arrows indicate the orientations of the contraction and dilatation axes of the basic deformation flow, respectively. The solid (dashed) double arrows also indicate the eddy orientations for extracting (losing) kinetic energy from (to) the mean flow optimally.

orientations elongated along the dilatation axis (dashed double arrows in Fig. 5) of the basic deformation and decay barotropically as they continue to deform to be further elongated along the dilatation axis due to the straining of the background deformation flow (Cai, 1992, 2003). The barotropic decay of HF eddies attributes to the weakening of HF variability in the jet exit region (Whitaker and Dole, 1995) and in both north and south flanks of the jet core. The net effect of HF eddies would act to broaden the jet in the meridional and downstream directions. By the same token, LF eddies, being mainly zonally elongated, decay barotropically in the jet entrance because they are elongated along the dilatation axis of the background deformation flow. They grow on the northern flank of the jet core and downstream

of the jet stream because their local orientations are along the local contraction axis of the background deformation flow. The stretching deformation in the jet exit region is the favorite (worst possible) place for a zonally (meridionally) elongated eddy to grow. This factor alone may explain why LF variability peaks further in the downstream portion and on the poleward flank of the jet streams, compared to its HF counterpart, and why there is a lack of HF variability in the jet exit region.

### 3.2. Baroclinic analysis

In this subsection we discuss the baroclinic energy conversion between the atmospheric transient eddies and the mean flow, based on the calculations using Eqs. (2) and (3). Figures 6 and 7 show the conversion of potential energy from the mean flow to perturbations for HF and LF transient eddies, respectively. Again, to facilitate discussions on the relation between eddy orientations and the basic stationary waves, we also evaluate the contributions to the total potential energy conversion from the  $x$ - and  $y$ -components of the inner products of the heat flux vector and the horizontal temperature gradient vector. Shown in panel (b)–(d) of Figs. 6–7 are the contributions from the west–east temperature contrast,  $-C_2 \overline{u'T' \frac{\partial T}{\partial x}}$ , from the zonal mean meridional temperature contrast,  $-C_2 \overline{v'T' \frac{\partial T}{\partial y}}$ , and from the meridional temperature contrast associated with stationary waves,  $-C_2 \overline{v'T' \frac{\partial T^*}{\partial y}}$ , respectively. The sum of the results of panel (b) through panel (d) of Figs. 6–7 equals that plotted in panel (a). It should be pointed out that unlike the barotropic energy conversion rate, the baroclinic energy conversion rate is not directly related to the (horizontal) orientation of eddies. As illustrated earlier, the zonally (meridionally) elongated eddies would amplify (decay) barotropically in the jet exit region. It follows that the preferred orientations of eddies would have a strong implication on the baroclinic energetic processes because of the strong zonal variation of the background baroclinicity associated with the stationary waves.

For HF transients, maximum potential energy conversion from the mean state occurs along the two major storm tracks (Figs. 1b and 6a). It is of interest to note that the magnitude of the potential energy conversion over the two storm tracks is similar despite that the Atlantic storm track is stronger than its North Pacific counterpart. It is also seen that the potential energy conversion is mainly associated with the meridional temperature contrast, in which the zonal mean part (Fig. 6c) is moderately larger than the stationary part (Fig. 6d).

The baroclinic energy conversion also plays an important role for LF eddies. As is the case of HF eddies, the zonally symmetric part of the time mean flow is the primary source for LF eddies (Fig. 7c). However, unlike HF eddies, the centers of baroclinic energy conversion to LF eddies due to the poleward heat fluxes of LF eddies (Figs. 7c–d) appear upstream of the maximum LF variability centers. Particularly, there is a substantial baroclinic energy conversion to LF eddies in the jet entrance region.

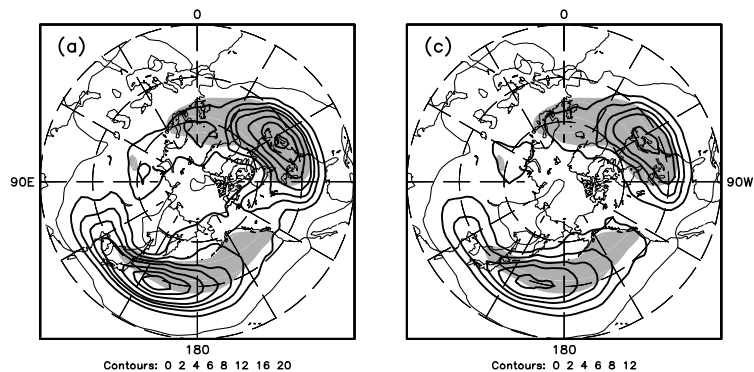


Fig. 6. Potential energy conversion rate (in units of  $W m^{-2}$ ) from the basic flow to HF transients: (a) total; (b) due to the west–east temperature contrast associated with stationary waves; (c) due to the zonal mean meridional temperature gradient and (d) due to the meridional temperature contrast associated with stationary waves (see text for the details of the partition of potential energy conversion rate). Shaded areas indicate the location of the storm tracks (HF standard deviation exceeds 60 m as shown in Fig. 1).

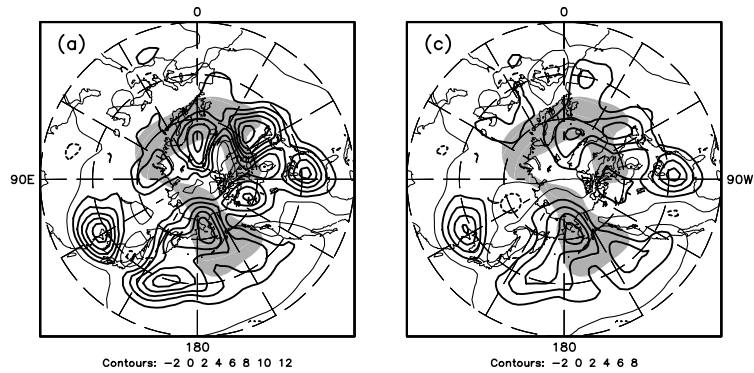
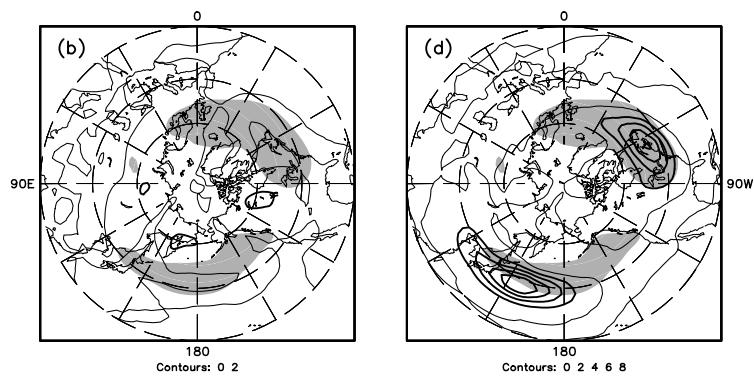
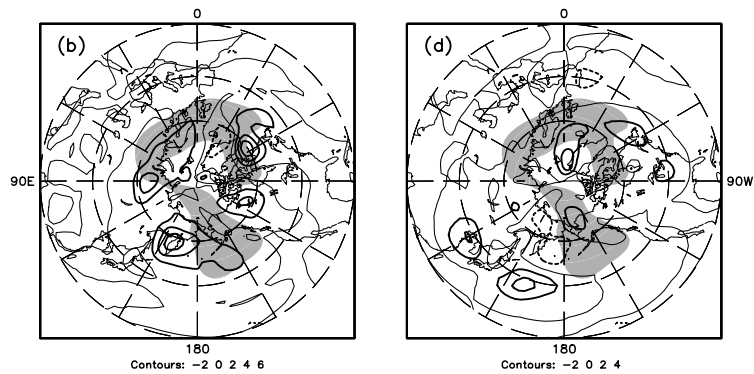


Fig. 7. Same as in Fig. 6, but for potential energy conversion rate from the basic flow to LF transients. Shaded areas indicate the regions where LF standard deviation exceeds 115 m as shown in Fig. 1.



It is the west–east temperature contrast associated with stationary waves that contributes to a substantial baroclinic energy conversion to LF eddies in the regions where the LF variability reaches the maximum (Fig. 7b). We attempt to relate the strong

down-gradient heat transport by LF eddies in the west–east direction to the preferred location of LF eddies, namely being further downstream from the jet core where the west–east temperature contrast is stronger. The net baroclinic energy conversion to LF

eddies (Fig. 7a) appears to have a broader spatial pattern, residing over both the storm track regions and maximum LF variability centres.

The conversion from eddy potential energy to kinetic energy for HF eddies suggests most of the potential energy gained by HF eddies from the mean flow is transferred into eddy kinetic energy (Fig. 8a), in accordance with baroclinic instability theory. However, the conversion from eddy potential energy to kinetic energy for LF eddies is strong only in the region where the storm

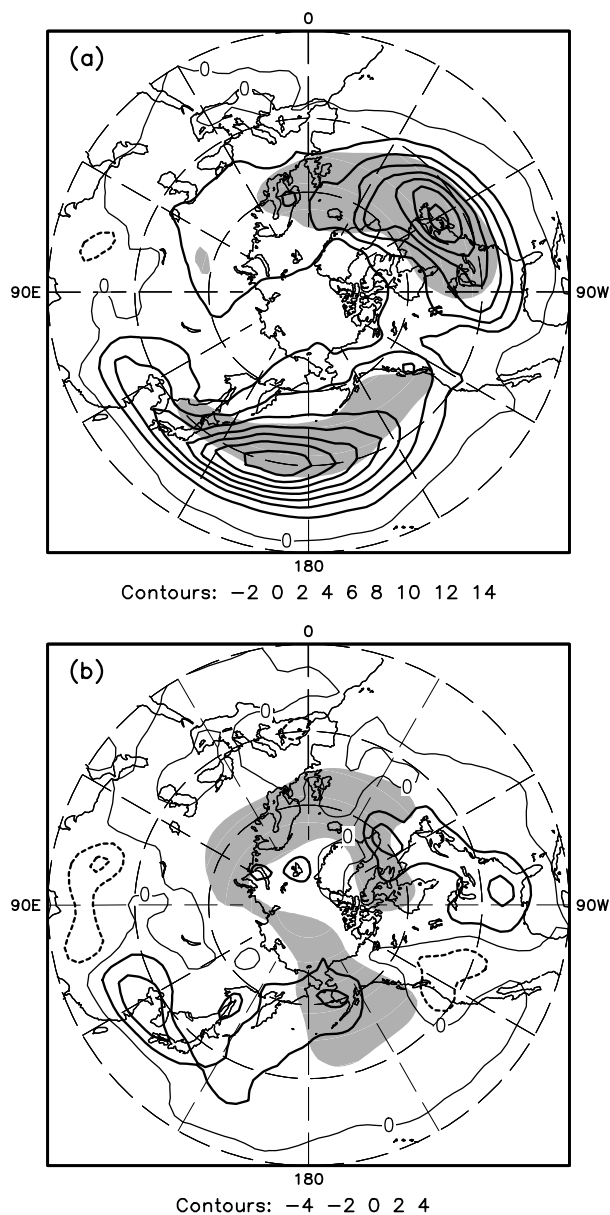


Fig. 8. Conversion rate (in units of  $\text{Wm}^{-2}$ ) from eddy potential energy to eddy kinetic energy for HF transients (a) and LF transients (b). Shaded areas indicate the regions where HF and LF standard deviation exceeding 60 and 115 m, respectively.

tracks are located (Fig. 8b). With reference to Fig. 7, the gain of potential energy by LF eddies in the storm track regions is mostly associated with the poleward heat fluxes (panels (c) and (d) of Fig. 7). The fact that there is little conversion from the potential energy gained by LF eddies into eddy kinetic energy in the regions where the LF variability tends to peak suggests that the underlying dynamical process for LF eddies to extract potential energy from the basic flow in these regions may not necessarily be associated with pure baroclinic instability. It is known that the leading internal sources of LF variability are the barotropic instability of the zonally varying flow (e.g. Simmons et al., 1983) and the symbiotic nonlinear interaction with HF eddies through upscale energy cascade (e.g. Cai and Mak, 1990b; Cai and van den Dool, 1991, 1992). According to Fig. 5b, the barotropic growth of LF eddies is strongest in the jet exit region due to their dominant zonally elongated orientation. Because of the presence of the background baroclinicity associated with the west–east temperature contrast of stationary waves in the jet exit region, LF eddies would inevitably gain potential energy from the basic flow by transporting heat down-gradient of the basic temperature gradient. This type of mixed barotropic–baroclinic energy extraction from the mean flow with little energy exchange between eddy potential and kinetic energy perhaps is a kind of ‘equivalent barotropic instability’ as described in Swanson (2000, 2001).

Displayed in Figure 9 are the mean amplitude of zonal wavenumber 1 through 10 of geopotential height and the phase difference between geopotential height and temperature fields (in degrees of its own wavelength) of both HF and LF eddies from  $20^\circ\text{N}$  to  $70^\circ\text{N}$ . It is seen that the amplitude of LF eddies (Fig. 9c) is nearly twice as large as that of HF eddies (Fig. 9a). Also it is clear that the scale separation in the temporal domain is reflected in the spatial domain in mid-latitudes since the largest amplitude of LF eddies lies in wavenumbers longer than four whereas the HF eddies have the largest amplitude in the synoptic waves with a wave number ranging from 5 to 7. Another important feature shown in Fig. 9 is that both LF and HF eddies have a westward tilting vertical structure and the westward tilting of LF eddies (Fig. 9d) is only slightly smaller than the HF eddies (Fig. 9b). This is consistent with the results presented in Fig. 7c, showing that the energy conversion rate of LF eddies from the potential energy of the zonal flow is nearly as large as that of HF eddies (Fig. 6c).

Both HF and LF eddies are trapped in the meridional waveguide following the westerly jet belt, implying that they have similar meridional scales. By the local Rossby wave dispersion relation, longer wavelength eddies would have lower frequencies. The results shown in Fig. 9 seem to suggest that there is little difference between HF and LF eddies as far as baroclinic energy conversion due to the poleward heat is concerned. However, the difference in the horizontal orientations between HF and LF eddies may have several important implications to their peak locations and their interaction with stationary waves. As summarized

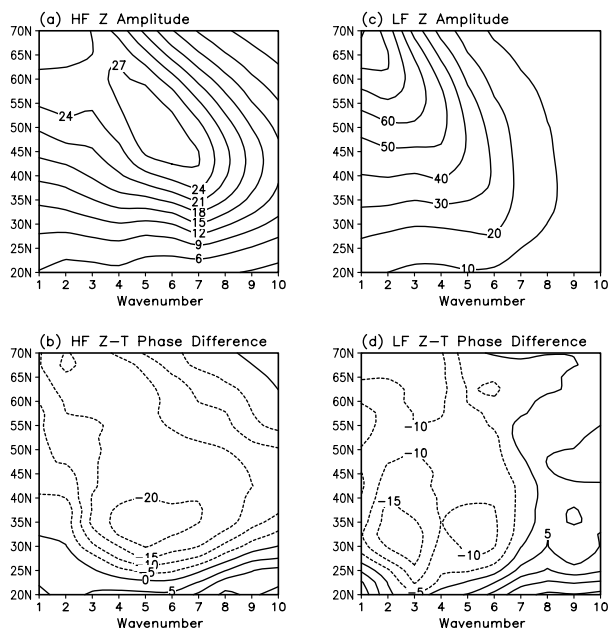


Fig. 9. The temporal mean amplitude (meters in the top panels) and westward tilting angle (degrees in the bottom panels) of transient eddies as a function of wavenumber (abscissa) and latitude (ordinate). The westward tilting angle is obtained as the mean phase difference between zonal harmonics in temperature and geopotential height anomalies of the same wavelength. A negative (positive) phase difference corresponds to the case where the temperature anomalies lag behind (lead ahead of) height anomalies and systems tilting to the west (east) in the vertical. Panels (a) and (b) are for HF amplitude and (c) and (d) for LF eddies.

in Fig. 5, the meridionally elongated HF eddies have a barotropic growth in the jet entrance region and a barotropic decay in the jet exit region. Within the jet core, the meridional temperature contrast associated with the stationary waves is strongest. As a result, the westward tilted and meridionally elongated HF eddies experience a rapid baroclinic growth while they pass through the jet stream. The barotropic decay helps to terminate the growth of HF eddies beyond the jet exit region. The zonally elongated LF eddies, on the other hand, have a barotropic growth in the jet exit region, but not in the jet entrance region. During their life cycle within the jet stream, they behave like HF eddies by having a westward tilting vertical structure. The westward tilting vertical structure ensures a baroclinic growth of LF eddies by extracting potential energy from the background flow and converting eddy potential energy to eddy kinetic energy. The barotropic growth of LF eddies in the jet exit region would act to extend their life cycle into the regions where the west–east temperature contrast associated with stationary waves is stronger such that they can grow both barotropically (Fig. 4b) and baroclinically (Fig. 7b) with little exchange between eddy potential and kinetic energy (Fig. 8b). The continuous growth of LF eddies due to both barotropic and baroclinic processes in the jet exit regions is consistent with the

facts that LF eddies reach maximum variability further downstream of the two major jet streams and that the LF variability is much stronger than HF eddies. Also the results seem to suggest that the notion of an equivalent barotropic structure perhaps is more meaningful only in the regions where the LF variability is maximal. Within the jet stream, the dynamical nature of LF eddies do not necessarily bear an equivalent barotropic structure as suggested in Figs. 7c–d and 8b showing a simultaneous conversion from the mean potential energy to eddies and from eddy potential energy to eddy kinetic energy along the jet stream.

### 3.3. Feedback of transient eddies

Using eqs. (6) and (7), we compute the geopotential height and temperature tendencies associated with the vorticity and heat transport of transient eddies. Although such calculations have been carried out numerous times in the literature (e.g. Lau and Holopainen, 1984; Cai and van den Dool, 1991, 1992; Lau and Nath, 1991), we here wish to relate the difference in the feedback fields between HF and LF eddies to their dominant orientations using a longer data record than used in previous studies. It is seen from Figs. 10a–b that both the mean height and temperature tendencies induced by meridionally elongated HF eddies exhibit a meridional dipole pattern over the east coasts. The polarity of the mean temperature tendency by HF eddies is opposite to the stationary waves whereas the height tendency is in phase with the stationary waves. Therefore, HF eddies act to maintain (damp) stationary waves by locally enhancing (reducing) north–south gradient of the height (temperature) field near the jet core regions. The eastward and northward shifting of the height tendency by HF eddies with respect to the stationary waves also implies that HF eddies act to shift the jet core poleward and downstream, in accordance with the barotropic energetics calculation shown in Fig. 3.

The time mean tendency fields induced by LF eddies, on the other hand, show a dominant zonal dipole wave pattern over the two coasts that is out of phase with the stationary waves (Figs. 10c–d). This suggests that LF eddies, being zonally elongated, act to primarily reduce zonal gradient associated with stationary waves both barotropically and baroclinically. The dominant dipole structure in the zonal direction of the LF feedback fields is consistent with our energetics calculation showing that LF eddies grow via both barotropic and baroclinic energy conversions primarily in the jet exit region where the west–east contrast of the stationary waves is strongest (Fig. 4b and Fig. 7b). It is of importance to note that the temperature feedback tendency due to LF eddies exhibits a weak dipole structure in the meridional direction that is opposite to the stationary waves. The meridional structure of the LF height feedback tendency, however, displays a dipole pattern that has the same polarity as the stationary waves. Therefore, the meridional pattern of LF feedback tendencies is very similar to that of HF eddies. This obviously is associated with the part of the life cycle when LF eddies pass through the jet

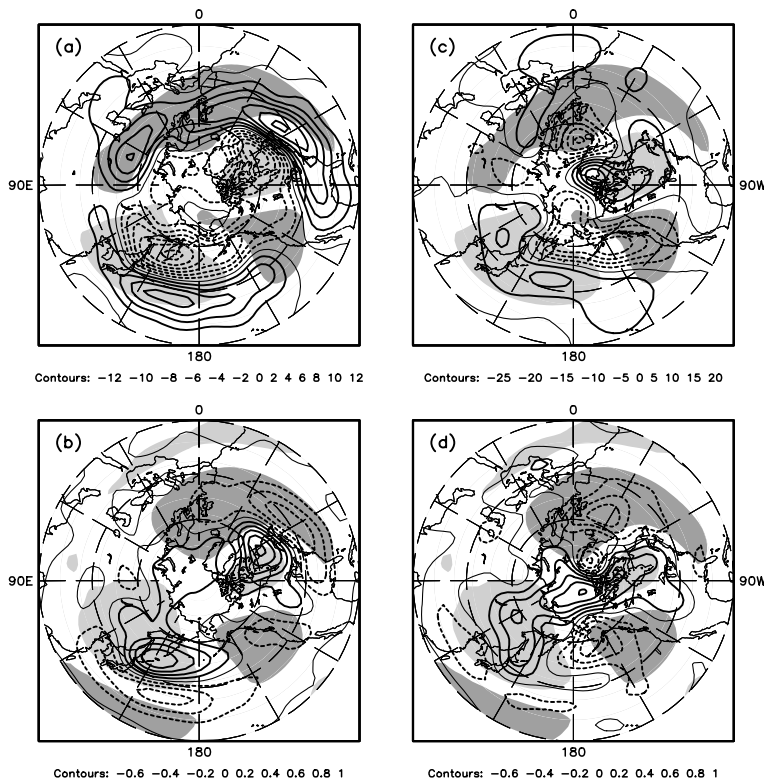


*Fig. 10.* Geopotential height tendency (top panels; meters per day) and temperature tendency (lower panels; °C per day) for HF variability (left-hand panels) and LF variability (right-hand panels), respectively. Shadings are indicative of stationary waves in 500-hPa geopotential height and temperature fields. Heavy shadings are for positive values and light shadings for negative values.

cores experiencing a growth that is primarily baroclinic nature as HF eddies.

#### 4. Summary

This study is focused on the question: what are the dynamical implications of eddy orientation in terms of the relation between the time-mean flow and the barotropic and baroclinic components? We address this question by diagnosing the energetics and feedbacks of both HF and LF eddies using the 53-yr (1948–2000) daily NCEP/NCAR Reanalysis. To exploit the relation between eddy horizontal orientations and the spatial variation of the background flow, we have evaluated the contributions to the total energetics of eddies from (1) the zonally averaged part of the mean flow, (2) the north–south contrast of the stationary waves and (3) the west–east contrast of the mean flow. Such a detailed energetics analysis enables us to examine how the spatial variations of the time mean state together with the dominant orientation of eddies determine the characteristics of the temporal variability of different time scales and their feedbacks onto the mean flow.

Wave decomposition analysis confirms that LF eddies in the extratropics are dominated by planetary scale waves whereas HF eddies are dominated by synoptic scale waves. This factor alone may explain why LF eddies have a zonally elongated orientation whereas HF eddies tend to be meridionally elongated assuming

that both HF and LF eddies have a similar scale in the meridional direction. Furthermore, the slower propagating phase speed for the same background wind speed due to a stronger westward retarded beta effect associated with a zonally longer wave may also explain why zonally longer waves are dominant with a longer time scale. We have also shown that both HF and LF eddies have a westward tilting vertical structure, implying that the familiar Lorenz energy cycle for baroclinic eddies is applicable to both HF and LF eddies.

Because of the strong zonal variation of the background deformation field along the jet stream and the difference in the horizontal orientations between LF and HF eddies, it is useful to discuss the difference or similarity between HF and LF eddies in two separate longitude sectors: one is with the jet core region and the other is jet entrance/exit regions. The energetics analysis shows that with the jet core region, LF eddies behave essentially the same as HF eddies. They grow baroclinically by transporting heat poleward and converting eddy potential energy to eddy kinetic energy. In terms of barotropic energy conversion in the jet core region, LF eddies also behave similar to HF eddies with some minor but noticeable differences. Specifically, LF eddies have a barotropic growth over the cyclonic shear side of the jet cores whereas the barotropic growth of HF eddies is confined to the north edge of the jet cores and HF eddies lose energy to the basic flow further north away from the jet core. Over the anticyclonic shear side of the jet cores, HF eddies lose kinetic energy

to the mean flow but LF eddies suffer little energy loss barotropically because their orientation lies between the contraction and dilatation axes of the basic deformation field.

However, the difference in the horizontal orientations between HF and LF eddies may have several important implications to their amplitude and peak locations, as well as their interaction with stationary waves. The meridionally elongated HF eddies have a barotropic growth in the jet entrance region and a barotropic decay in the jet exit region. The barotropic decay acts to terminate the growth of HF eddies beyond the jet exit region. The zonally elongated LF eddies decay barotropically in the jet entrance regions but can grow barotropically in the jet exit region. Therefore, even though LF eddies behave like HF eddies during their life span within the jet core, they continue to grow in the jet exit region. The growth of LF eddies in the jet exit region comes from two sources: a barotropic growth due to the straining of the background deformation flow and a baroclinic growth due to the down-gradient heat flux by LF eddies across the west–east temperature contrast associated with stationary waves. The continuous growth of LF eddies due to both barotropic and baroclinic processes in the jet exit regions is consistent with the observations that LF eddies reach maximum variability further downstream of the two major jet streams and that the LF variability is much stronger than HF eddies. It is of interest to note that the growth of LF eddies in the jet exit region seems to involve little exchange between eddy potential and eddy kinetic energy.

The results of the energetics analysis are confirmed by the feedback analysis, showing that HF eddies, being dominated by meridional orientations, mainly act to maintain (damp) stationary waves by locally enhancing (reducing) north–south gradient of the height (temperature) field near the jet core regions. The zonally elongated LF eddies, on the other hand, act to primarily reduce zonal gradient associated with stationary waves both barotropically and baroclinically.

## 5. Acknowledgments

The authors thank Dr. K.-M. Kim, NASA Goddard Space Flight Center, for his assistance in application of the Hanning filter. The authors are grateful to Drs. Peitao Peng and Shuntai Zhou for their valuable suggestions on the first draft of the paper. The insightful comments and suggestions from the two anonymous reviewers helped to improve the presentation greatly. Ming Cai was supported by grant GC04-163 from the NOAA Office of Global Programs.

## References

- Andrew, D. G. 1983. A conservation law for small-amplitude quasi-geostrophic disturbances on a zonally asymmetric basic flow. *J. Atmos. Sci.* **40**, 85–90.
- Black, R. X. 1998. The maintenance of extratropical intraseasonal transient eddy activity in the GEOS-1 assimilated dataset. *J. Atmos. Sci.* **55**, 3159–3175.
- Black, R. X. and Dole, R. M. 2000. Storm tracks and barotropic deformation in climate models. *J. Climate* **13**, 2712–2728.
- Blackmon, M. L., Wallace, J. M., Lau, N.-C. and Mullen, S. L. 1977. An observational study of the northern hemisphere wintertime circulation. *J. Atmos. Sci.* **34**, 1040–1053.
- Branstator, G. W. 1995. Organization of stormtrack anomalies by recurring low-frequency circulation anomalies. *J. Atmos. Sci.* **52**, 207–226.
- Cai, M. 1992. A physical interpretation for the stability property of a localized disturbance in a deformation flow. *J. Atmos. Sci.* **49**, 2177–2182.
- Cai, M. 2003. Local instability dynamics of storm tracks. *Observation, Theory and Modeling of Atmospheric Variability*, eds X. Zhu, and co-editors, World Scientific, Singapore, pp. 3–38.
- Cai, M. and Mak, M. 1990a. On the basic dynamics of regional cyclogenesis. *J. Atmos. Sci.* **47**, 1417–1442.
- Cai, M. and Mak, M. 1990b. Symbiotic relation between planetary and synoptic scale waves. *J. Atmos. Sci.* **47**, 2953–2968.
- Cai, M. and van den Dool, H. M. 1991. Low-Frequency waves and traveling storm tracks. Part I: Barotropic component. *J. Atmos. Sci.* **48**, 1420–1436.
- Cai, M. and van den Dool, H. M. 1992. Low-Frequency waves and traveling storm Tracks. Part II: Three-dimensional structure. *J. Atmos. Sci.* **49**, 2506–2524.
- Chang, E. K. M., Lee, S.-Y. and Swanson, K. L. 2002. Storm track dynamics. *J. Climate* **15**, 2163–2183.
- Cressman, G. F. 1981. Circulations of the West Pacific jet stream. *Mon. Wea. Rev.* **109**, 2450–2463.
- Cressman, G. F. 1984. Energy transformation in the East Asia–West Pacific jet stream. *Mon. Wea. Rev.* **112**, 563–571.
- Cuff, T. J. and Cai, M. 1995. Interaction between the low- and high-frequency transients in the Southern Hemisphere winter circulation. *Tellus* **47A**, 331–350.
- Dole, R. M. and Black, R. X. 1990. Life cycle of persistent anomalies. Part II: The development of persistent negative height anomalies over the North Pacific Ocean. *Mon. Wea. Rev.* **118**, 824–846.
- Edmon, H. J., Hoskins, B. J. and McIntyre, M. E. 1980. Eliassen–Palm cross section for the troposphere. *J. Atmos. Sci.* **37**, 2600–2616.
- Egger, J. and Schilling, H.-D. 1983. On the theory of the long-term variability of the atmosphere. *J. Atmos. Sci.* **40**, 1073–1085.
- Farrel, B. F. 1989. Transient development in confluent and diffluent flow. *J. Atmos. Sci.* **46**, 3279–3288.
- Hanning, R. W. 1983. Kaiser windows and optimization. In *Digital Filters* 2nd Edition (R. W. Hanning), 257 pp.. Prentice-Hall, Inc., Englewood Cliffs, New Jersey, United States, 167–187.
- Held, I. M., Lyons, S. W. and Nigam, S. 1989. Transients and the extratropical response to El Niño. *J. Atmos. Sci.* **46**, 163–176.
- Hoskins, B. J., James, I. N. and White, G. H. 1983. The shape, propagation and mean-flow interaction of large-scale weather systems. *J. Atmos. Sci.* **40**, 1595–1612.
- Iacono, R. 2002. Local energy generation in barotropic flows. *J. Atmos. Sci.* **59**, 2153–2163.
- Kalnay, E., Kanamitsu, M., Kistler, R., Collins, W., Deaven, D. and co-authors, 1996. The NCEP/NCAR 40-Year Reanalysis Project. *Bull. Amer. Meteor. Soc.* **77**, 437–471.
- Kistler, R., Kalnay, E., Collins, W., Saha, S., White, G. and co-authors, 2001. The NCEP/NCAR 50-year reanalysis. *Bull. Amer. Meteor. Soc.* **82**, 247–268.

- Lau, N.-C. 1988. Variability of the observed midlatitude storm tracks in relation to low-frequency changes in the circulation pattern. *J. Atmos. Sci.* **45**, 2718–2743.
- Lau, N.-C. and Holopainen, E. O. 1984. Transit eddy forcing of the time-mean flow as identified by geopotential tendencies. *J. Atmos. Sci.* **41**, 313–328.
- Lau, N.-C. and Nath, M. J. 1991. Variability of the baroclinic and barotropic transient eddy forcing associated with monthly changes in the midlatitude storm tracks. *J. Atmos. Sci.* **48**, 2589–2613.
- Limpasuvan, V. and Hartmann, D. L. 1999. Eddies and the annular modes of climate variability. *Geophys. Res. Lett.* **26**, 3133–3136.
- Limpasuvan, V. and Hartmann, D. L. 2000. Wave-maintained annular modes of climate variability. *J. Climate* **7**, 1144–1163.
- Mak, M. and Cai, M. 1989. Local barotropic instability. *J. Atmos. Sci.* **46**, 3289–3311.
- Peng, S. and Whitaker, J. S. 1999. Mechanisms determining the atmospheric response to midlatitude SST anomalies. *J. Climate* **12**, 1393–1408.
- Plumb, R. A. 1986. Three-dimensional propagation of transient quasi-geostrophic eddies and its relationship with the eddy forcing of the time mean flow. *J. Atmos. Sci.* **43**, 1657–1678.
- Robinson, W. A. 1991. The dynamics of low-frequency variability in a simple model of the global atmosphere. *J. Atmos. Sci.* **48**, 429–441.
- Sheng, J. and Derome, J. 1991. An observational study of the energy transfer between the seasonal mean flow and transient eddies. *Tellus* **43A**, 128–144.
- Simmons, A. J., Wallace, J. M. and Branstator, G. W. 1983. Barotropic wave propagation and instability, and the atmospheric teleconnection patterns. *J. Atmos. Sci.* **40**, 1362–1392.
- Shutts, G. J. 1983. The propagation of eddies in diffluent jetstreams: Eddy vorticity forcing of “blocking” flow fields. *Quart. J. Roy. Meteor. Soc.* **109**, 737–761.
- Swanson, K. L. 2000. Stationary wave accumulation and generation of low-frequency variability on zonally varying flows. *J. Atmos. Sci.* **57**, 2262–2280.
- Swanson, K. L. 2001. Blocking as a local instability to zonally varying flows. *Quart. J. Roy. Meteor. Soc.* **127**, 1341–1355.
- Swanson, K. L. 2002. Dynamical aspects of extratropical tropospheric low-frequency variability. *J. Climate* **15**, 2145–2162.
- Swanson, K. L., Kushner, P. J. and Held, I. M. 1997. Dynamics of barotropic storm tracks. *J. Atmos. Sci.* **54**, 791–810.
- Takaya, K. and Nakamura, H. 2001. A formulation of a phase-independent wave-activity flux for stationary and migratory quasi-geostrophic eddies on a zonally varying basic flow. *J. Atmos. Sci.* **58**, 608–627.
- Ting, M. 1994. Maintenance of northern summer stationary waves in a GCM. *J. Atmos. Sci.* **51**, 3286–3308.
- Ting, M. and Held, I. M. 1990. The stationary wave response to a tropical SST anomaly in an idealized GCM. *J. Atmos. Sci.* **47**, 2546–2566.
- Watanabe, M. and Kimoto, M. 2000. On the persistence of decadal SST anomalies in the North Atlantic. *J. Climate* **13**, 3017–3028.
- Whitaker, J. S. and Dole, R. M. 1995. Organization of storm tracks in zonally varying flows. *J. Atmos. Sci.* **35**, 1265–1280.